JOURNAL OF OPTOELECTRONICS AND ADVANCED MATERIALS Vol. 9, No. 1, January 2007, p. 134 - 140

Invited Lecture

Charge transport in organic materials: From molecular wire to 3D systems

S. NEŠPŮREK, P. TOMAN, M. MENŠÍK, I. KRATOCHVÍLOVÁ[a], J. SWORAKOWSKI[b], T. MALLOUK[c]
Institute of Macromolecular Chemistry, Academy of Sciences of the Czech Republic, Heyrovský Sq. 2, 162 06 Prague 6, Czech Republic
[a]Institute of Physics, Academy of Sciences of the Czech Republic, Na Slovance 2, 182 21 Prague 8, Czech Republic
[b]Institute of Physical and Theoretical Chemistry, Wroclaw University of Technology, Wyb. Wyspianskiego 27, 50-370 Wroclaw, Poland
[c]Department of Chemistry, The Pennsylvania State University, University Park, PA 16802, U.S.A

The main limitation on the charge carrier mobility in polymer-based molecular wires follows from polaron formation and the dispersion of transfer integrals among the monomer units. The electrical current passing through a single molecule is influenced by charge tunnelling – the Fowler-Nordheim model seems to be a good approximation for the description of charge transport. The presence of dipolar species results in a mobility decrease, due to the increase of the transfer integral dispersion. Polar groups, chemically attached to the molecular wire, can causeorbital localization. The charge transport in 3D samples can be described by the theory of disordered polarons, which postulates that the activation energy of the charge carrier mobility is composed of contributions both from the dynamic disorder, i.e. the polaronic barrier, and from the static disorder, i.e. the variation of the energy of transport states as a result of the environment. The main contribution to the polaron binding energy results from molecular deformation; the electron-phonon term makes only a 5 % contribution. Dipolar additives make the distribution of hopping states broadened and new localized states for charge carriers are formed which results in a reduction of the charge mobility.

(Received November 28, 2006; accepted December 21, 2006)

Keywords: Charge transport, Molecular wire, Polaron, Charge mobility

1. Introduction

Current research in molecular physics focuses, among other things, on the design and implementation of nanometer scale electronic systems, which exhibit new classical and quantum mechanical effects. The motivation for creating such elements has been two-fold: first, to create nanoscale laboratories to explore physics in a new way, and second, to develop novel devices with significant applications.

The architecture of molecular-scale electronic devices can be designed, starting from molecular segments whose properties have been known from experiment and/or suitable theoretical models. Some examples of molecules or nanostructures that might be used as switching units, memories, logic elements and devices embodying a negative resistance have recently been demonstrated (e.g., [1-4]). A pioneering construction of a molecular switch was based on the electron tunnelling principle [1]. Recently, Chen et al. [5] proposed a new type of electrical switch embodying a negative resistance based on a two-step reduction process occurring on a molecular wire containing a donor-acceptor substituent, 2'-amino-4,4'-di(ethynylphenyl)-5'-nitro-1-benzene-1-thiol. As the voltage is increased, the molecular wire initially undergoes a one-electron reduction at the location of the donor-acceptor unit, thereby supplying a charge carrier for electron flow through the system. A further increase in the voltage causes a second electron reduction, with subsequent blocking of the current. However, detailed studies by Donhauser et al. [3] showed that the switching is due to conformational changes in the molecule or bundles, rather than to the electrostatic effects of charge transfer.

One of the most important parameters for molecular wires is charge transport. In this paper, we present the basic principles of charge carrier transport in 1D systems, including charge tunnelling, polaron formation and the influence of acceptors and dipolar groups on charge carrier movement. For comparison, these effects are also discussed in 3D systems, where hopping transport of disordered polarons is important.

2. Experiment

In this Section, we will briefly mention materials and physical methods, which were utilized for the acquisition of the results mentioned below.

(I) $HS-(CH_2)_n-COOH$ (TMA)

10-sulfanyldecanoic acid (n = 9)
16-sulfanylhexadecanoic acid (n = 15)

(II) 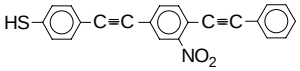

(NDR)

4-{[3-nitro-4-(phenylethynyl) phenyl]ethynyl} benzene-1-thiol

(III) 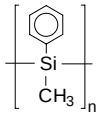

(PMPSi)

Poly[methyl(phenyl)silylene]

(IV) 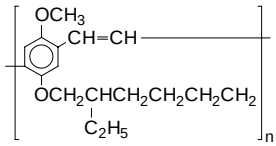

(MEH-PPV)

Poly({2-[(2-ethylhexyl)oxy]-5-methoxy-1,4-phenylene}vinylene)

(V) 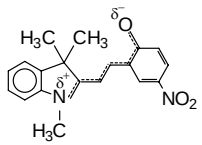

(MR)

4-nitro-2-[2-(1,3,3-trimethyl-3*H*-indol-1-ium-2-yl)vinyl]phenoxide

(VI) 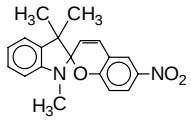

(SP)

6-nitro-1',3',3'-trimethylspiro[chromene-2,2'-indoline]

Fig. 1. Molecular materials under investigation.

The current-voltage ($j \sim U$) characteristics were measured using a HP 4155 semiconductor parameter analyzer. Measurements of the "on-chain" charge carrier mobility were carried out using time-resolved microwave photoconductivity (TRMP) [6]. Photocurrent measurements were performed by the time-of-flight (TOF) technique [7]. TRMP measurements were performed on powder samples, TOF and $j \sim U$ measurements on sandwich metal-insulator-metal configurations.

Rod-shaped nanowires (TMA, NDR) were prepared in the system of 70 nm diameter pores of polycarbonate truck etched membranes [8]. The bottom Au contact was electroplated and the self-assembled monolayer of the active molecules was attached in an alkaline medium through a thiol-bridge. The top gold electrode for the sandwich configuration was prepared by metal-vapour deposition to the H terminated molecules. After these procedures, the membrane was dissolved. The molecular cluster was 7 μm long.

Quantum mechanical modelling was performed using the Hartree-Fock/3-21 G(*) method and the Grozema et al. [9] uncorrelated CED – type technique.

3. Charge transport in molecular wires

3.1. "Quasi-single" molecule system

There are not many published results concerning charge transport in single "quasi-single" molecules. Mbindyo et al. [8] put forward experimental current-voltage characteristics ($j \sim U$) measured on samples of Au|TMA|Au. They were nearly symmetrical with voltage polarity. A strong nonlinearity was observed for voltages higher than 1 V. The electrical current for the molecule with n = 9 (see (I) in Fig. 1) was about 10^{-13} A at 1.5 V. The increase of the number of CH_2 groups in the molecule made the current value lower, viz., for n = 15 a current of 10^{-13} A was reached at about 3 V [8]. It is assumed that Au creates good Ohmic contact to organics. Thus, the current flowing through the sample is mainly influenced by the bulk properties of the material and the contact barrier. It was possible to fit the experimental current-voltage characteristics by the Fowler-Nordheim approximation for charge tunnelling. According to this model, the current j can be written as

$$j(U) \approx \frac{U^2}{d^2} \exp\left(-\frac{Kd\varphi^{3/2}}{U}\right) \tag{1}$$

$$K = \frac{8\pi\sqrt{2m^*}}{3eh} \tag{2}$$

where U is the applied voltage, d is the barrier thickness (here, the length of the molecule), φ is the barrier height, m^* is the effective mass of the charge carrier, e is the elementary charge and h is Planck's constant.

For the fitting of experimental data, it is necessary, first, to estimate the effective mass of the charge carrier. To overcome this problem, a sample of the type Au|TMA|Ag was prepared. Thus, after the application of voltages of different polarities, the charge carriers must overcome two different barriers. One can calculate the derivative

$$\alpha_i = \frac{\mathrm{d}[\ln(jU^{-2})]}{\mathrm{d}U^{-1}} = -Kd\varphi^{3/2} \tag{3}$$

where i = 1,2 for different types of electrode. These equations allow us to determine the pre-contact barrier heights. Assuming that electron injection is limited by the precontact barrier

$$\varphi = \left|\phi_m - A_g\right| \tag{4}$$

where ϕ_m is the work function of the metal and A_g is the electron affinity of the molecule, from the ratio α_1/α_2 one can get the value of the electron affinity. The barriers, determined for Au|TMA, n = 9 and Au|TMA, n = 15 interfaces, were found to be φ = 2.1 eV (d = 15 Å, n = 9) and φ = 2.0 eV (d = 19 Å, n = 15), respectively. These values are close to the literature data. Since, for both

materials, the barrier heights are nearly the same, this suggests that the barrier height is not very sensitive to the chain length. When a conjugated molecule (NDR, see (II) in Fig. 1) is used instead of (I), the current increases by 5 orders of magnitude, being influenced by the presence of delocalized π-electrons in the molecule. The presence of an electron accepting nitro-group on the central phenyl gave rise to the region of negative resistance on the $j \sim U$ characteristic.

3.2. Determination of the mobility of charge carriers on a molecular wire

The "on-chain" charge carrier mobility can be determined by time resolved microwave conductivity (TRMC) or photoconductivity (TRMP). Here, we will demonstrate the results obtained by TRMP on a PMPSi ((III) in Fig. 1) molecular wire, where charge carrier transport is enabled due to σ-conjugation.

Excitation at 355 nm in PMPSi results in the formation of electron-hole pairs in the Si backbone that undergo a fast chain geminate recombination to a significant extent. The remaining portion of the ion pairs escape fast geminate recombination, presumably due to the fact that σ-conjugation extents only over a limited number of silicon atoms, with the consequence that only electron-hole pairs formed in the same conformational chain segment can recombine fast. The remainder of the electron-hole pairs relax to the ion-pair (σ, π*) charge-transfer state. This implies a transfer of the electron from the silicon backbone to the pendant phenyl groups.

A TRMP trace measured on PMPSi powder [10] is shown in Fig. 2. The signal shows a dispersive behaviour: at least two components of the decay can be distinguished. The initial rapid decay signal, with a half-life of $\tau_{1/2}$ = (80 ± 20) ns, is followed by a slow process. The kinetics of the latter part of the signal can be fitted with a stretched exponential function, up to the millisecond range.

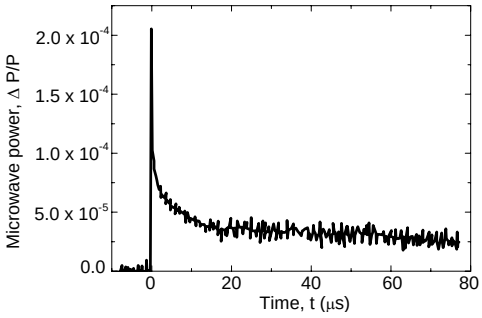

Fig. 2. TRMP trace for PMPSi; λ_{exc} = 355 nm.

For the homogeneous diffusion-controlled recombination of electrons and holes, the recombination half-life τ_R is given by the relation

$$\tau_R = \frac{\varepsilon\varepsilon_0}{e\mu N} \tag{5}$$

where $\varepsilon\varepsilon_0$ is the electric permittivity, μ is the charge mobility and N is the pair concentration. Taking τ_R (= $\tau_{1/2}$) from the fast part of the experimental kinetics (N was determined by calibration of the microwave signal using TiO_2), one can estimate the value of the on-chain mobility as 2×10^{-6} m^2 V^{-1} s^{-1}, in good agreement with the data presented in [11]. This value is very probably still limited by conformational disorder and structure defects in the backbone. In alkyl-substituted polysilylenes, the hole mobilities seem to increase with increasing length of the substituent; e.g., in poly[hexyl(phenyl)silylene], an "on-chain" mobility of 2×10^{-5} m^2 V^{-1} s^{-1} was reported [12]. The long-time decay process can be related to intra-chain recombination (hole on Si chain, electron localized on phenyl) and/or to interchain electron-hole recombination. The value of the charge carrier mobility must be, in this case, close to the zero-field drift mobility measured on 3D samples, as was indeed observed (at room temperature μ ($F \rightarrow 0$) ≈ 10^{-9} m^2 V^{-1} s^{-1} [13]; from measurements of the microwave conductivity, 2×10^{-9} m^2 V^{-1} s^{-1} was obtained [11]).

Note that the "on-chain" mobilities in π-conjugated carbon polymers are usually higher (up to 7 $\times 10^{-5}$ m^2 V^{-1} s^{-1}). For MEH-PPV (see (IV) in Fig. 1), the value $\mu = 10^{-7}$ m^2 V^{-1} s^{-1} was found by TRMC pulse-radiolysis [14]. Lower "on-chain" mobilities in σ-conjugated molecular wires, in comparison with π-conjugated ones, can be attributed to a greater conformational disorder and a decrease in the overall electronic coupling, due to lower barriers to conformations other than all-trans.

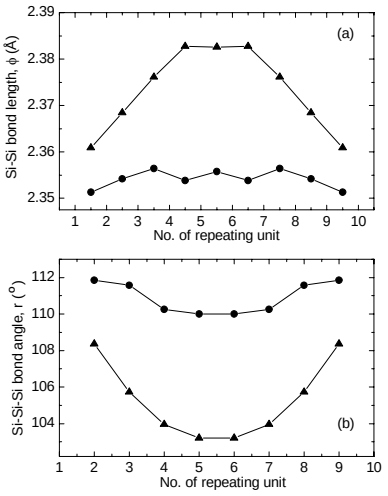

Fig. 3. Calculated changes of the Si–Si bond lengths (a), and the Si–Si–Si bond angles (b) during positive polaron formation (▲) in deca[methyl(phenyl)silylene]; symbols (●) are for the neutral chain.

A question arises as to why the values of the "on-chain" mobilities are so low. A possible reason is a polaron formation. The strong electron-phonon coupling causes carrier self-trapping and creates a quasiparticle, a polaron, which can move only by carrying along the associated molecular deformation. The motion of such a

charge carrier, dressed in a cloud of local deformation of the nuclear subsystem, can be phenomenologically described by introducing a temperature-dependent effective mass, which is higher than the electron mass. A significant distortion of the PMPSi chain was detected found by Kim at al. [15] by measuring the migration rate of the excitation energy along the polymer chain. These observations were supported by quantum-chemical calculations [6] (see Fig. 3).

Another important feature influencing the charge movement on the molecular wire is the presence of traps. Let us assume an assembly of non-interacting chains, forming a regular primitive lattice, the inter-chain distance amounting to a. Let us further consider a single infinite chain allowing the transport of charge carriers, containing defects at an average distance l from one another, which form localized states of depth E_t. Thus, the volume concentration of these traps (n_0) will amount to

$$n_0 = \left(a^2 l\right)^{-1} \tag{6}$$

The balance of carriers at a trap is determined by two rates: the rate of supply (r_s)

$$r_s = a^2 n_f \mu F \tag{7}$$

and the rate of release (r_t equal to the inverse of the trapped carrier lifetime, τ_t)

$$r_t = \tau_t^{-1} = \nu \exp\left(-\frac{E_t}{kT}\right) \tag{8}$$

In the above equations, n_f, F and ν stand for the concentration of free carriers, the field intensity and the frequency factor, respectively, T is the temperature and k is the Boltzmann constant. It should be noted, at this point, that the field dependencies of some characteristic parameters might differ from those valid in 3D systems [16,17]. In particular, ν is field dependent at low fields (up to 10^6 V m^{-1}).

The current density will be given by

$$j = \frac{e}{a^2} r \tag{9}$$

where r = min (r_s, r_t). Thus, two regimes should be expected: at low supply rates (i.e., low voltages) the current obeys the usual equation

$$j = e n_f \mu F \tag{10}$$

whereas at high voltages the current will be limited by the rate of detrapping

$$j = \frac{e\nu}{a^2} \exp\left(-\frac{E_t}{kT}\right) \tag{11}$$

In strictly 1D systems, one should expect dramatic changes of the currents resulting from the possible creation or annihilation of traps (vide infra). For example, switching between traps of depths of 0.5 and 1 eV should result in an on/off ratio of the order of 10^8.

3.3. Theoretical modeling of charge transport in molecule wires, and the influence of the external electric field – a molecular FET device

The charge mobility in a π-conjugated molecular wire of poly({2-[(2-ethylhexyl)oxy]-5-methoxy-1,4-phenylene}vinylene) (MEH-PPV (IV) see Fig. 1), was modelled by the tight-binding approximation. The polymer chain was represented by a sequence of N sites (alternating phenylenes and vinylenes), corresponding to the repeat units. The charge carrier motion in such a chain can be described by the Hamiltonian (non-dissipative model)

$$H = \sum_{n=1}^{N} \left[\varepsilon_n a_n^+ a_n - b_{n,n+1}\left(a_{n+1}^+ a_n + a_n^+ a_{n+1}\right)\right], \tag{12}$$

where a_n and a_n^+ are the annihilation and creation operators of a charge carrier at an n-th site, ε_n is the energy of a charge carrier localized at this site, and $b_{n,n+1}$ is the transfer integral between the sites n and n+1. Using this Hamiltonian, with the molecular parameters ε_n and $\beta_{n,n+1}$ and the hole wave function $|\psi(t)\rangle$, taken in the form of a linear combination of the states located at the individual sites, the time-dependent Schrödinger equation

$$i\hbar \frac{\partial}{\partial t} |\psi(t)\rangle = H |\psi(t)\rangle \tag{13}$$

can be numerically integrated (note that at time t = 0, the hole was assumed to be localized on a single unit in the middle of the chain). Subsequently, one may calculate the mean-square displacement $\Delta^2(t)$ of the charge carrier, defined by the relation

$$\Delta^2(t) = \langle \psi(t) | n^2 | \psi(t) \rangle \, b^2 \tag{14}$$

where b is the inter-unit distance (3.35 Å in the case of MEH-PPV). This quantity, in (14), is related to the frequency dependent intramolecular ("on-chain") charge carrier mobility $\mu(\omega)$ by the Kubo formula [18]

$$\mu(\omega) = \frac{-e\omega^2}{2kT} \mathrm{Re}\left[\int_0^\infty \Delta^2(t) \exp(-i\omega t) dt\right] \tag{15}$$

For the diffusive motion, which is expected in the long time limit due to destructive interference even in the non-dissipative model, $\Delta^2(t) = 2Dt$. In this case, the Kubo formula can be rewritten in the form of the Einstein relation

$$\mu(\omega \to 0) = \frac{e}{2kT} \cdot \frac{\Delta^2(t)}{t} = \frac{eD}{kT} \tag{16}$$

where D is the diffusion coefficient.

Grozema et al. used this approach for the calculation of the hole mobility in poly(phenylene vinylene) and polythiophene [12]. They calculated the distribution of the transfer integrals $b_{n,n+1}$ from the torsional disorder of the polymer chain and neglected the energetic disorder of ε_n, assuming the same site energy for all repeating units of the same type. For an infinite MEH-PPV chain, they found the mobility value extrapolated to the zero frequency $\mu(\omega \to 0)$ to be 2×10^{-5} m^2 V^{-1} s^{-1}, which is a little higher than the published experimental value obtained from the microwave conductivity [14].

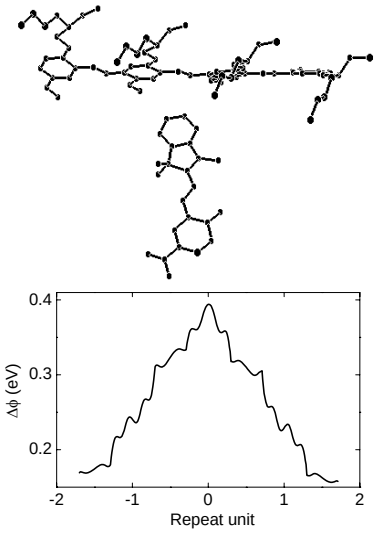

Fig. 4. The change of the on-chain electrostatic potential of a MEH-PPV tetramer, caused by the additive molecule (V).

We extended this model for the calculation of the charge carrier mobility in a polymer doped by a polar additive. Polar species modify the on-chain electrostatic potential, due to charge–dipole interactions. The model situation for the MEH-PPV and polar additive (V), is shown in Fig. 4. The change of the electrostatic potential shifts the site energies of the polymer repeating units, and consequently the polymer transport levels are modified. If the positions and orientations of the additive molecules, with respect to the polymer chain, are essentially random, the effect results in a broadening of the distribution of transport states. The most important parameter of this distribution is its half-width, which can be approximated by the standard deviation $\sigma(\varepsilon)$ of the site energies from its average value (energetic disorder).

Taking into account that the additive molecules cannot be placed very close to the polymer chain, due to the presence of substituents, it is possible, at a first approximation, that the additive molecules can be considered as randomly distributed and mutually oriented non-interacting point dipoles (the minimal distance of the dipoles from the polymer chain was taken to be 1 nm). In the point dipole approximation, the standard deviation $\sigma(\varepsilon)$ is proportional to the additive dipole moment and square root of the additive concentration. For MEH-PPV highly doped by an MR additive ((V), 12 D, ca. 20 %wt), the standard deviation $\sigma(\varepsilon)$ was calculated as 0.37 eV, while for the additive ((VI), dipole moment 6 D) $\sigma(\varepsilon)$ was 0.18 eV. Numerical calculation of the on-chain charge carrier mobility, using the above described technique, shows that the introduction of energetic disorder with a standard deviation $\sigma(\varepsilon)$ = 0.37 eV leads to a decrease in the mobility by two orders of magnitude, in comparison with the undoped case. Note that charge-phonon coupling was neglected.

A qualitatively different situation arises when a polar molecule is chemically attached through a spacer [–CO–C(H)OH] to the molecular wire. The model calculations were performed on a PMPSi wire with a side group of SP type (see Fig. 1, structure (VI)). Under illumination by UV light the SP moiety forms a metastable merocyanine structure MR (structure (V) in Fig. 1). As polysilane is a hole-transporting material, chemical traps affecting the charge transport are expected to occur on sites with locally modified ionization energies. Because an isolated molecular wire behaves as a one-dimensional system where there is no scattering, both the increase and decrease in the ionization energy should result in the formation of local states on the molecular wire.

The formation of local states for holes, during the photochromic transformation SP $\rightarrow$ MR, can also be inferred from the characters of the orbitals, as follows from Fig. 5. The HOMO of a polymer substituted by a SP group is localized on the main chain, as well as the HOMO of an unsubstituted polymer; thus, hole transport in the polymer wire is possible. After the photo-transformation of the side group and dipole formation, the molecular orbitals are reordered, and consequently the HOMO is localized on the MR side group (see HOMO-LOC"M" in Fig. 5).

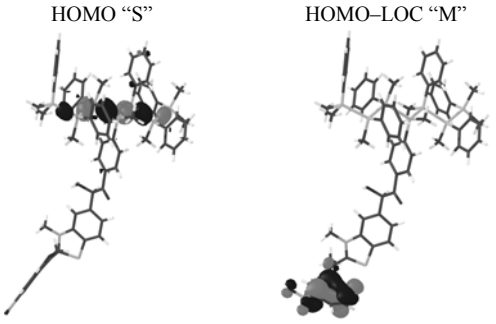

Fig. 5. HOMO orbitals of the PMPSi molecular wire during the SP $\rightarrow$ MR photo-transformation of the side group.

The charge is localized, and carrier transport is impeded. The situation is similar to that presented in Section 3.1. To be re-activated to the main chain, the charge should overcome the potential barrier between the highest molecular orbital localized on the main chain and the HOMO-LOC"M", which amounts to several tenths of aneV. Alternatively, it can tunnel between the side groups

of the molecular wire, provided the inter-site distances are sufficiently short.

4. Charge carrier transport in 3D samples

Three-dimensional (3D) thin films of PMPSi are used as model materials for further discussion.

Figure 6 illustrates the dependences of the charge carrier mobility, μ, of a PMPSi sandwich sample (thickness ca. 2 μm) on F, the electric field strength, at different temperatures. In all cases, the mobility can be described by an exp ($\beta F^{1/2}$) dependence for $F > 10^7$ V m^{-1}. At lower field strengths, $\mu(F)$ becomes constant or increases slightly upon reducing F. This behaviour [13] is in agreement with the data published by Bässler et al. [19]. These types of dependences are usually treated in the framework of the hopping disorder concept. The essential difference between the polaron and disorder models is that the latter, at variance with the former, implies a sufficiently weak electron-phonon coupling and the activation energy of charge transport reflects the static energy disorder of the hopping sites. In contrast, the polaron model suggests a strong electron-phonon coupling and molecular deformation; the contribution of energy disorder to the activation energy of the carrier mobility is negligible.

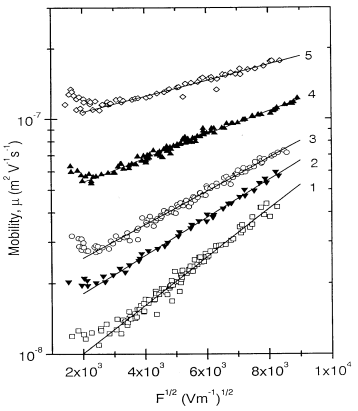

Fig. 6. Electric field dependence of the mobility of PMPSi, parametric in temperature: T = 295 K (curve 1), 312 K (curve 2), 325 K (curve 3), 355 K (curve 4), 358 K (curve 5).

Since the structural distortion is an intra-molecular process, the polaron binding energy E_p is not subjected to meaningful variation. Concomitantly, the polaronic charge transport must obey Gaussian statistics, and the photocurrent transients should neither feature a long tail nor become dispersive at any temperature. However, these predictions were not confirmed experimentally in polymers. In addition, the small polaron model fails to account for the observed Poole-Frenkel-type field and non-Arrhenius temperature dependences of the thermal-equilibrium carrier mobility. It was suggested [13,19,20] that the zero-field activation energy of the mobility, E_a ($F \rightarrow 0$), can be approximated by the sum of the disorder and polaron contributions as

$$E_a(F \rightarrow 0) = E_a^{pol} + E_a^{dis} = \frac{E_p}{2} + \frac{4}{9}\frac{\sigma^2}{(kT)} \quad (17)$$

where E_a^{pol} and E_a^{dis} are the polaronic and disorder contributions and σ is the energy width of the density of states (DOS) distribution. Thus, the activation energy should be temperature dependent and if the disorder term prevails, one should obtain a non-Arrhenius temperature dependence. Based on experimental data, however it is usually difficult to decide whether a μ ($1/T^2$) or μ ($1/T$) dependence is fulfilled.

The polaron binding energy was determined for PMPSi as E_p = 0.16 eV, from the temperature dependence of the activation energy of the mobility [19]. Taking into account the field and temperature dependencies of the mobility, fitting of the experimental data resulted in E_p = 0.28 eV, using theory based on the effective medium approach [20]. Model quantum chemical calculations gave the value E_p = 0.23 eV. Note that this value consists of the charge-phonon contribution, which is about 0.01 eV, and the deformation term (about 0.22 eV), which includes molecular deformation of the molecule during the polaron formation, charge redistribution and polarization.

It is not simple to experimentally detect the polaron formation. One possibility is using the technique of thermo-stimulated luminescence (TSL) TSL [21]. The method is based on the fact that TSL measurements are performed after some dwell time on samples, which have been photo-excited at liquid helium temperature, and the initial distribution of polarons is formed in the course of low-temperature energy relaxation. Polaron formation strongly affects both the low-temperature energy relaxation and the thermally assisted hopping of charge carriers in a disordered material. If the polaron binding energy is comparable to or larger than the DOS width, energetically downward hopping is strongly suppressed by the lack of deeper vacant sites, which are only accessible for further jumps at low temperatures. Therefore, after a fast initial polaronic relaxation, the energy distribution of polarons remains almost "frozen in" over the entire dwell time between the low-temperature photo-excitation of the sample and the onset of the TSL heating run. With increasing temperature, energetically upward polaron jumps become the dominant hopping mode, and these jumps control the TSL kinetics. The polaronic contribution to the activation energy of every individual upward jump is equal to *half* the polaron binding energy, $E_p/2$, while the low-temperature energy relaxation of polarons within the DOS distribution is slowed down because the polaron energy distribution is shifted down by E_p. This leads to a stronger polaronic effect on the low-temperature relaxation than on the thermally stimulated hopping. Therefore, at moderate values of E_p , the polaronic effect shifts the TSL peak to lower temperatures, as compared to its position for a material with a similar DOS width and with E_p = 0. Thus, the polaron occurrence can be treated by additional infrared (IR) irradiation after photoexcitation and before the TSL run measurement. This results in the shift of the

TSL peak towards higher temperatures, and in a decrease its intensity [21].

Similarly to the case of a molecular wire, charge carrier transport in 3D systems is strongly influenced by polar additives. Electron-dipole interactions influence the value of the polarization energy, which results in two effects: (i) broadening of the distribution of hopping states, and (ii) formation of new localized states for charge carriers. Both effects reduce the value of the charge carrier mobility.

5. Conclusions

Interconnection (by polymeric wires in molecular electronics) of elements in electronic circuits represents an important step in device technology. Charge carrier transport involves charge delocalization and tunnelling. The latter process can be modelled by the Fowler-Northeim approximation. Polar species attached to the molecular wire as side groups are responsible for the orbital and charge localization, which limits the charge carrier movement; in some special cases a region of negative resistance can appear on the current-voltage characteristic. Polar species in the vicinity of the molecular wire make the distribution of electron states broadened, due to the electron-dipole interactions; this results in the reduction of the charge mobility. Similar effects can be observed in 3D materials. Here, the charge transport can be described by the model of disordered polarons, which postulates that the activation energy of the charge carrier mobility is composed of contributions both from the dynamic disorder, i.e., the polaronic barrier, and the static disorder, i.e., the variation of the energy of transport states as a result of the environment. The polaron binding energy consists of a charge-phonon contribution (5 %), and a term related to the molecular deformation and polarization during polaron formation (95 %).

Acknowledgements

The work was sponsored by the Grant Agency of the Academy of Sciences of the Czech Republic (grant No. KAN 401770651 and No. A401770601), by the Ministry of Education, Youth and Sports (grant No. 1041/2006-32 – COST), and by the Polish Ministry of Science (grant No. 3 T08E 084 30).

References

[1] F. L. Carter (Ed.), Molecular Electronic Devices, M. Dekker, New York, 1982.
[2] S. Nešpůrek, J. Sworakowski, IEEE Eng. Medicine Biol. **13,** 45 (1994).
[3] Z. J. Donhauser, B. A. Mantooth, K. F. Kelly, L. A. Bumm, J. D. Monnell, J. J. Stapleton, D. W. Price Jr., A. M. Rawlett, D. L. Allara, J. M. Tour, P. S. Weiss, Science **292,** 2303 (2001).
[4] S. Nešpůrek, J. Sworakowski, Thin Solid Films **393**, 168 (2001).
[5] J. Chen, M. A. Reed, A. M. Rawlett, J. M. Tour, Science **286,** 1550 (1999).
[6] S. Nešpůrek, P. Toman, J. Sworakowski, Thin Solid Films **438-439**, 268 (2003).
[7] S. Nešpůrek, H. Valerián, A. Eckardt, V. Herden, W. Schnabel, Polym. Adv. Technol. **12,** 306 (2001).
[8] J. Mbindyo, N. Kovtynkhova, B. Razavi, I. Kratochvílová, S. Augelo, T. Mayer, T. Jackson, T. Mallonk, High-dielectric Ceramics **223**, 155 (2002).
[9] F. C. Grozema, P. T. van Duijnen, Y. A. Berlin, M. A. Ratner, L. D. A. Siebbeles, J. Phys. Chem. B **106,** 7791 (2002).
[10] S. Nešpůrek, V. Herden, M. Kunst, Schnabel, Synth. Met. **109,** 309 (2000).
[11] H. Frey, M. Möller, M. P. de Haas, N. J. P. Zenden, P. G. Schouten, G .P. van der Laan, J. M. Warman, Macromolecules **26,** 89 (1993).
[12] F. C. Grozena, L. D. A. Siebbeles, J. M. Warman, S. Seki, S. Tagawa, U. Scherf, Adv. Mater. **14,** 228 (2002).
[13] S. Nešpůrek, A. Eckhardt, Polym. Adv. Technol. **12**, 427 (2001).
[14] G. H. Gelinck, J. M. Varman, E. G. J. Staring, J. Phys. Chem. **100**, 5485 (1996).
[15] Y. R. Kim, M. Lee, J. R. G. Thorne, R.M. Hochstrasser, J. M. Zeigler, Chem. Phys. Lett. **145,** 75 (1988).
[16] J. Sworakowski, G. F. Leal, Ferreira, J. Phys. D: Appl. Phys. **17**, 135 (1984).
[17] E. G. Wilson, Chem. Phys. Letters **90**, 221 (1982).
[18] R. Kubo, J. Phys. Soc. Japan, **12,** 570 (1957).
[19] H. Bässler, P. M. Borsenberger, R. J. Perry, J. Polym. Sci. B: Polym. Phys. **32,** 1677 (1994).
[20] I. I. Fishchuk, A. Kadashchuk, H. Bässler, S. Nešpůrek, Phys. Rev. B **67**, 224303 (2003).
[21] V. I. Arkhipov, E.V. Emelianova, A. Kadashchuk, I. Blonsky, S. Nešpůrek, D. S. Weiss, H. Bässler, Phys. Rev. B **65**, 165218 (2002).

*Corresponding author: nespurek@imc.cas.cz